

Article

Suitability and Sustainability of Anti-Graffiti Treatments on Natural Stone Materials

Valentina Roviello ^{1,*} , Aurelio Bifulco ¹ , Abner Colella ² , Fabio Iucolano ¹ , Domenico Caputo ¹ , Antonio Aronne ¹ and Barbara Liguori ¹ 

¹ Department of Chemical, Materials, and Industrial Production Engineering (DICMaPI), University of Naples Federico II, Piazzale V. Tecchio 80, 80125 Naples, Italy; aurelio.bifulco@unina.it (A.B.); fabio.iucolano@unina.it (F.I.); domenico.caputo@unina.it (D.C.); anaronne@unina.it (A.A.); barbara.liguori@unina.it (B.L.)

² Department of Earth, Environment and Resources Sciences, University of Naples Federico II, Via Cintia 21, 80126 Naples, Italy; abner.colella@unina.it

* Correspondence: valentina.roviello@unina.it; Tel.: +39-346-644-4862

Abstract: Graffiti vandalism represents an aesthetic and structural phenomenon of degradation both for buildings and cultural heritage: the most used sprays and markers can permeate the stone materials exposing them to degradation. Hence, great attention is being currently devoted to new non-invasive chemical approaches to face this urgent problem. This work is aimed at deeply examining the effects of some of the most sustainable chemical protective methods on the physical properties of natural building materials (e.g., tuff and limestone) by testing two commercial anti-graffiti products. It was found that the nanotechnological product Ector (E) was more effective than Nord Resine (NR) in anti-graffiti applications even if its permanent character hinders its application to the cultural heritage. Conversely, the less performant NR could be used in this field due to its sacrificial behavior, according to the guidelines of the Italian Ministry of Cultural Heritage and Activities and Tourism. The findings highlight the importance of developing new sustainable methods for the preservation of cultural and building materials from vandal graffiti, which should combine the high hydrophobia, the ecological characteristics, and the effectiveness of E, with the sacrificial properties of NR.

Keywords: vandal graffiti; anti-graffiti products; sustainable chemical methods; alteration of stone materials; tuff; limestone; cleaning tests; spray; markers



Citation: Roviello, V.; Bifulco, A.; Colella, A.; Iucolano, F.; Caputo, D.; Aronne, A.; Liguori, B. Suitability and Sustainability of Anti-Graffiti Treatments on Natural Stone Materials. *Sustainability* **2022**, *14*, 575. <https://doi.org/10.3390/su14010575>

Academic Editor: Asterios Bakolas

Received: 15 December 2021

Accepted: 3 January 2022

Published: 5 January 2022

Publisher's Note: MDPI stays neutral with regard to jurisdictional claims in published maps and institutional affiliations.



Copyright: © 2022 by the authors. Licensee MDPI, Basel, Switzerland. This article is an open access article distributed under the terms and conditions of the Creative Commons Attribution (CC BY) license (<https://creativecommons.org/licenses/by/4.0/>).

1. Introduction

Graffiti vandalism or graffiti writing is a phenomenon of urban decay born as a subversive act towards the social, economic, and political system. Over time this phenomenon became an instrument enabling graffiti writers to obtain considerable visibility, having sometimes criminal connotations, punishable by the law [1]. The illegal nature of graffiti vandalism is associated with the serious risk of damaging not only the building walls. Heavily graffitied urban areas assume increasingly negative reputations, since graffiti-rich areas are often labeled as socio-economically poor [2]. Lastly, and most importantly, it damages the historical-architectural heritage. Writers use different techniques to realize their signatures (or *tags*), that are an expression of their groups; one of the most important is the technique called *tar*, which was imported from Marseille (France) and is currently reported also in some Italian cities. The *tag* is made with sprays and markers sometimes composed by bituminous paint to create very shiny 3D writings. This *tar tag* dries very slowly and can easily make dirty the support where is applied [1]. Many monuments, statues, artistic installations, facades of historical buildings are placed at risk by the application of *tags* with different kinds of commercial paints, including those modified by writers, that can penetrate inside materials with a highly receptive and absorbent surface. Also, staining varnishes being easily carried by solvents, and it can penetrate deeply by altering the

micro-structure of the materials, making cleaning operations particularly difficult, exposing them to atmospheric agents and further degradation. Several cleaning methods are usually used, the choice of which depends mainly on two factors: the means used (spray paints, markers) and the kind of material object of vandalism (i.e., natural, or artificial stone and materials with different porosity and surface properties) [3]. Since the 1990s, conservation scientists have been searching for solutions and methodologies to remove graffiti from buildings and monuments safely and selectively as well as effective anti-graffiti products to protect surfaces of artistic interest, that prevent the adhesion of paint layers [4]. There are several removal methods currently in use that can be grouped for simplicity in three classes: physical-mechanical, biological, and chemical. Innovative physical-mechanical techniques for the removal of vandal graffiti include laser ablation technology, ultrasonic agitation, plasma spray or thermal removal [4–7]. Other methodologies make use of jets of water at high pressures, sand blasting, air blasting [8], though these techniques are generally economically not sustainable. These techniques and others related to them should be avoided especially in the treatment of items of high value [5], as they can cause surface wear and micro-fractures leading to a further increase in the roughness and therefore the permeability of stone materials. The biological methods use microorganisms which can remove graffiti through biodegradation [9–11]. Among the chemical methods, there are growing examples of new products for the removal of graffiti paints based on solvent mixtures directly applied onto materials or dispersed in inert adsorbent media. Chemical methods are also used to protect surfaces by using commercial and synthetic anti-graffiti inorganic-organic based compounds, such as resins, waxes, and polymers [3,12–14]. Among all the above methods, the chemical ones are the most promising, especially in the case of synthetic products which comply with the standards in the field of cultural heritage. When choosing the most suitable product, one must consider the characteristics of the material to be protected and ensure the use of products having a minimum chromatic interference and maximum reversibility, and not classified as “permanent”. According to the guidelines released by the Italian Ministry for Cultural Heritage and Activities and for Tourism, these products must be accompanied by a data sheet describing their chemical class and reversibility characteristics, the percentage of the active substance, as well as the compatibility of the product with other materials and the application and removal procedures [5]. While the phenomenon of vandal graffiti is growing steadily and affects many types of widely studied materials, including marble, travertine, concrete, natural stone, and limestone, [7,8], current studies are focused mainly on the protection/consolidation of tuff [15,16]. On the other hand, there is a lack of studies on the performances of anti-graffiti products on tuff and Vicenza stone. In this research work, we studied the effect of two anti-graffiti products in the first place on the preservation and then the removal of vandal graffiti on two natural stones, Viterbo red tuff and Vicenza stone. In particular, the preservation of tuff and, thus, the choice of a suitable anti-graffiti is very challenging, due to the extremely heterogeneous and highly porous morphology of this stone. The Vicenza stone was also selected in this investigation because it was widely used by the major Italian sculptors and architects for the realization of artworks since the Renaissance [17]. Moreover, we studied not only the effectiveness of the anti-graffiti products, but also the compatibility between the product and the substrates, to assess if the treatment had sacrificial or permanent results and if the removal of the coating left the morphology, the color, and the chemical-physical properties of the natural stones unchanged. Finally, we evaluated the efficiency of a sustainable cleaning methodology at a microscopic level, simulating the action of writers with graffiti sprays and markers (acrylic and bituminous based). The cleaning method using high-pressure water was avoided because it could damage the porous materials, as has also been reported in the literature [18], and, thus, all samples were cleaned by using warm water [2,14].

2. Materials and Methods

2.1. Materials

Two substrates were used for this research: the Viterbo red tuff (the so-called “Vico red tuff with black scoria”) and the Vicenza stone, two natural stone materials, with different composition, porosity, properties, and use. In detail, the Viterbo red tuff (Central Italy) is a lithoid ignimbrite characterized by textural and mineralogical heterogeneous nature and a high porosity, strongly zeolitized (mainly chabazite with a minor amount of phillipsite) with black juvenile scoriaceous clasts and crystals in a cineritic matrix which usually tends to a yellow reddish color [19], with good mechanical properties, used generally in construction and paving. The Vicenza stone is a sedimentary rock from Veneto region (Northern Italy), which is characterized by an ivory white color. It is a limestone low in silica and clay, with rare Fe-oxides and hydroxide, organogenic (composed by foraminifera, red algae and corallinae algae) cemented by microcrystalline calcite ($\text{CaCO}_3 > 99\%$ by volume), characterized by variable fine to coarse grain size and high porosity (ca. 28% in volume) [20–22]. It was widely used in the past in ornamentation and sculpture for columns, tympanums, stairways for garden furnishings, and statues [20]. Given the different use of the materials and the various surface characteristics of roughness, higher in the first compared to the second case, these two materials are targeted differently by vandals: sprays could more easily applied on Viterbo tuff surfaces, while a mix of sprays and markers can be applied on the Vicenza stone that has a smoother surface on which it is easier to write. Both these materials (called “T” and “VS”, respectively), provide a good test bench for this research as representative natural stone materials, widely used for public buildings and cultural heritage.

2.2. Anti-Graffiti Products

Two commercial anti-graffiti products were studied: one permanent, Ector RG-10 (here simply indicated as “Ector” or “E”), a nanotechnological and environmentally sustainable product (<https://www.ectorlab.com/rr-group/>, accessed on 3 December 2021), and a semi-sacrificial anti-graffiti Nord Resine (indicated simply as “Nord Resine” or “NR”). The first is defined as a hybrid mixture based on SiO_2 nanoparticles in aqueous solution, ecological and breathable, indicated as an ideal treatment for different surfaces: historical monuments, natural and artificial stones, porous and non-porous stones. The second product is an aqueous suspension of organic-inorganic hybrid compounds, ideal for a wide range of materials: porous and non-porous materials, natural and artificial and one semi-sacrificial product. Based on exhaustive research, we found that these anti-graffiti products are the most innovative in the market, particularly for natural and porous stones, and have been chosen because of their different compositions and typologies. All the chemical details are reported in Table 1. According to the EC Regulation [23] both commercial products are classified as not dangerous. The anti-graffiti products were applied with a brush with soft bristles, according to the recommendations listed in the technical sheets (in details for porous materials Ector has been applied pure and a second crossing coat made within 2–3 min from the first application; Nord Resine has been applied first diluted 1:1 and then pure), then left at laboratory conditions for 24 h.

Table 1. Commercial anti-graffiti used; all details were obtained from the data and security sheets.

Product	Description	Type	Density (g/cm^3)	pH	Boiling Point ($^{\circ}\text{C}$)	Dynamic Viscosity (mPas)
Ector RG-10 (R. & R. Group SRL)	Mixture of modified hybrid materials based on SiO_2 nanoparticles in aqueous solution.	Permanent	1.0 ± 0.03 (20 $^{\circ}\text{C}$)	3–5	>100	1–10
Anti-graffiti (Nord Resine S.p.A.)	Aqueous suspension of hybrid organic/inorganic compounds	Semi sacrificial	1.00 ± 0.02 (20 $^{\circ}\text{C}$)	5.0	>100	-

2.3. Graffiti Paints

Three commercial aerosol spray paints were used: noir brilliant (Colors Motip Dupli, RAL 9005) and blue cobalt (Colors Motip Dupli, RAL 5013) spray paint, bitumen black spray (Montana Cans, Tar Black Low-Pressure), bitumen black marker (Molotow Coversall™ Signal Black 660PI). The first two spray paints are acrylic, and diesel based, while the last one was oil (bitumen) based. These sprays and markers have been selected in this work because they are different in composition, and because the oil-based product is difficult to remove, and there are no previous studies reported in the literature.

2.4. Sample Preparation

Both stone materials were cut with a water saw by using a diamond blade to obtain tiles of (10 × 10 × 2) cm. The specimens were cleaned to remove any remaining dirt, then placed in the oven at 40 °C until constant weight was attained. Then they were characterized before and after the treatments with anti-graffiti and paints. After coating with graffiti paints in the laboratory, the tiles were left for over 1 month at room temperature and finally subjected to the cleaning test, following the technical data sheets.

2.5. Characterizations of Products/Materials

The chemical properties of the anti-graffiti products were investigated by means of FT-IR infrared spectrometry (Spectrum 3, Universal ATR sampling accessory, Perkin Elmer). The pipe method, as reported in the European Standard UNI EN 16302 [24] consists in the use of a Karsten tube. This technique was useful to measure the water absorption on the surface of porous inorganic materials under low pressure, to simulate the pouring rain conditions and to estimate the efficacy of the anti-graffiti treatments [25]. The Colorimetric test (CM-2500d Konica Minolta spectrophotometer, Konica Minolta sensing Europe B.V., Milan, Italy) was performed, according to European Standard UNI EN 15886 [26], to verify the stone chromatic changes on the untreated surface and after the brushing treatment with the anti-graffiti products. The color variation of the surface is not generally perceived by the human eye if ΔE (total color differences) is <3 , while when $\Delta E > 5$, an observer can clearly recognize different colors on the examined surface [25]. Therefore, a ΔE of 5 can be considered as the maximum threshold value generally accepted as chromatic alteration for stones that undergo coating/consolidation treatments [27]. The ΔE values obtained is the average of 10 different points of the same surface. Static contact angle analysis was performed according to UNI EN 15802 [28] to assess the hydrophobic properties of the anti-graffiti products. The homemade test equipment consists of a Digital Microscope (Dino-Lite Premier 2 AD4113T (R4), ANMO Electronic Corporation) provides a digital visualization and at one time a source of illumination of drop. The digital microscope is equipped also with a software (Dino Capture 2.0) that allows the manual measurement of θ contact angles. The micro flat-head pipette (Gilson P20) is a high precision droplet dispensed volume (10 μ L). For morphologic observations, small specimens were put on aluminum stub with graphite adhesive and metalized with Au and Pd to highlight differences on the surface of the stone materials before (blank) and after treatments with graffiti paints and secondly only with anti-graffiti products. The Scanning Electron Microscope is a Nova NanoSem 450 (FEI/Thermofisher Scientific US). All the SEM micrographs were acquired at 50 μ m and at 10 μ m (5 kV, using EDT detector), to better appreciate morphological differences. A cleaning test was performed to evaluate the protection efficiency of the anti-graffiti products on the natural stone materials before and after treatments with paints and the effectiveness of cleaning with hot water (60 °C). Since sacrificial anti-graffiti products are removed usually during the cleaning process with the paints, semi-permanent products can be removed after a few (two or three) cycles of cleaning and the permanent anti-graffiti can withstand repeated cleaning cycles [18]. Here, both the semi-sacrificial and the permanent products, have undergone two cleaning cycles, after which it is possible to appreciate visible improvements of surface cleanliness. The pictures collected are micro-photographs (12.8×) captured with a digital microscope.

3. Results and Discussion

3.1. FT-IR Infrared Spectrometry

In order to determine the main classes of chemical constituents of the two anti-graffiti products, we first conducted a characterization using FT-IR infrared spectrometry. In Figure 1, the FT-IR spectra for the analyzed formulations (E and NR) are reported. Both spectra show infrared bands occurring at 2860 cm^{-1} and 2970 cm^{-1} (stretching vibration of the C–H in unsaturated moieties) [29], at 1020 cm^{-1} (mono- and para-substituted benzene derivatives) [30], at 802 cm^{-1} and 871 cm^{-1} (aromatic C–H stretching in para and ortho, respectively) [29,31]. Consequently, it may be possible to affirm that E and NR are mainly based on epoxy resins as polymer binder systems.

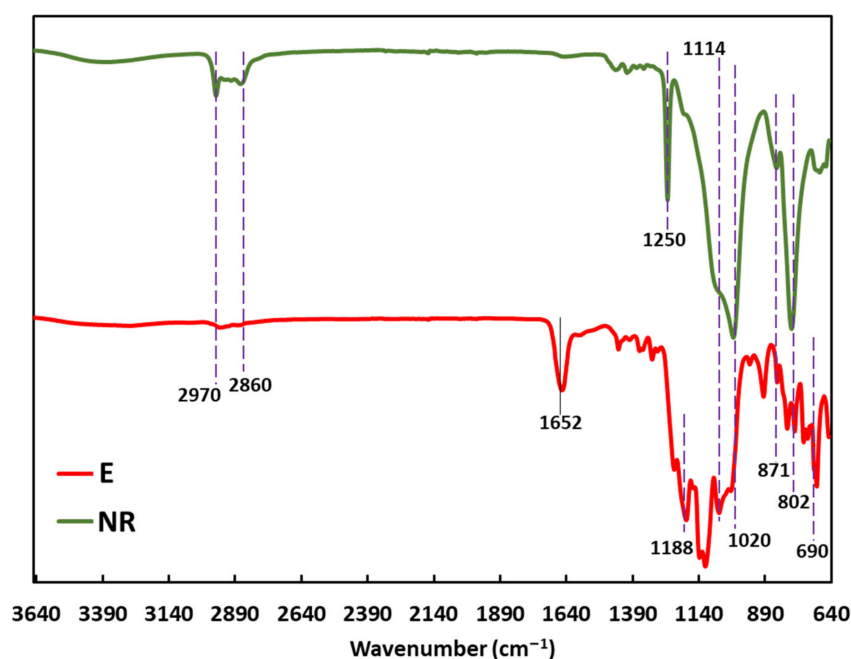


Figure 1. FT-IR spectra of investigated products: E and NR.

Moreover, the band at 1114 cm^{-1} is due to Si–O stretching and discloses the use of silica nanoparticles as fillers in both formulations [32,33]. For the E system, the band at 1188 cm^{-1} (in-plane CH deformations) suggests the presence of a silane agent, which may contain halo-atoms (X), since the band stretching at 690 cm^{-1} is normally ascribed to C–X groups [34]. The band at 1652 cm^{-1} (C–H bending of aromatic moieties) [29], is probably due to the presence of a solvent in E formulation. On the contrary, the lack of this band in the NR system together with the band at 1250 cm^{-1} (C–N stretching) [31] suggests that there are not any halo-based silane agents but rather nitrogen containing ones, which may act as coupling agents for silica nanoparticles. The above FT-IR analysis is in good agreement with the reported chemical composition in the labels of both commercial formulations.

3.2. Chromatic Modifications

A colorimetric analysis was performed (Figure 2) to appreciate the possible chromatic variations of the stone surfaces after anti-graffiti coatings.

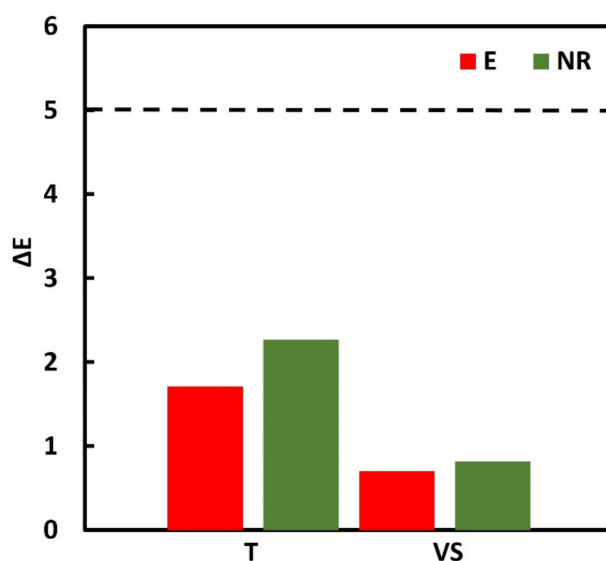


Figure 2. Colorimetric analysis: total color changes (ΔE) for the brushing treated samples of T and VS, with E and NR. Dotted line highlights the threshold value of $\Delta E = 5$.

It was gratifying to observe that commercial products did not cause chromatic changes: ΔE values were found always less than 3 and, therefore, the color changes are not visible to the human eye. Moreover, $\Delta E < 5$ ensures their compliance with the pertaining regulations. This is more evident with NR than E, that shows a slight increase of ΔE for red T when compared to VS.

3.3. Morphological Observations and Static Contact Angle Characterization

The T samples were covered on the surface with graffiti paints and subsequently examined by SEM (Figure 3) to verify the alteration of stone morphology. We chose T as representative material as, being endowed with higher roughness and heterogeneity than VS, it showed better morphological evidence.

The morphology of the stone material was observed before (blank in a), with Spray paints coating (Motip Dupli black in b, Montana Cans Tar Black in c), and with the bitumen black marker (Molotow in d). The sprays seem to leave the morphology of the materials almost unchanged if compared with the untreated sample (a), and the texture and mineralogy of tuff is still recognizable. On the contrary, the marker (d) forms a film altering completely the morphology that appears rather uniform and with a low surface roughness. The bitumen marker is a very complex mixture consisting of molecules with various and high molecular weights (which add waterproof, sticky [35] and highly viscous properties) that fail to pass through the pores of the materials on which the marker is deposited. As observed in Figure 3d, this kind of marker forms a compact film, making even the roughest stone material, such as tuff, uniform and smooth. This suggests that the removal of markers should be more difficult compared to all sprays. However, one should not underestimate the removal difficulties related to the sprays that being conveyed by the connectivity of pores necessitate difficult cleaning processes. SEM observations after stone were treated with anti-graffiti products are shown in Figures 4 and 5. In addition, higher magnification (10 μm) SEM micrographs of Figures S1 and S2 in Supplementary Materials show more detailed morphologies for VS and T, respectively. Also, in Figure 4d,e the static contact angle analyses are reported. The untreated VS surface (Figure 4a) shows irregular and almost characteristic rhombohedral calcite crystals with a porous surface morphology [20,22,36].

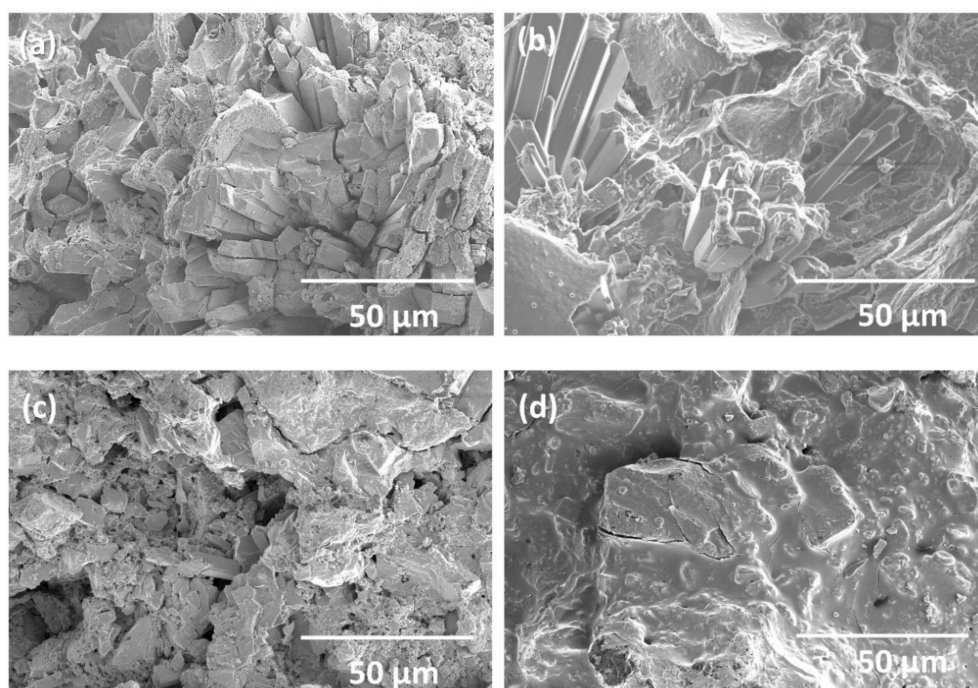


Figure 3. SEM micrographs of T before (a) and after coating with spray Colors Black (b), spray Montana Cans (c) and marker Molotow (d).

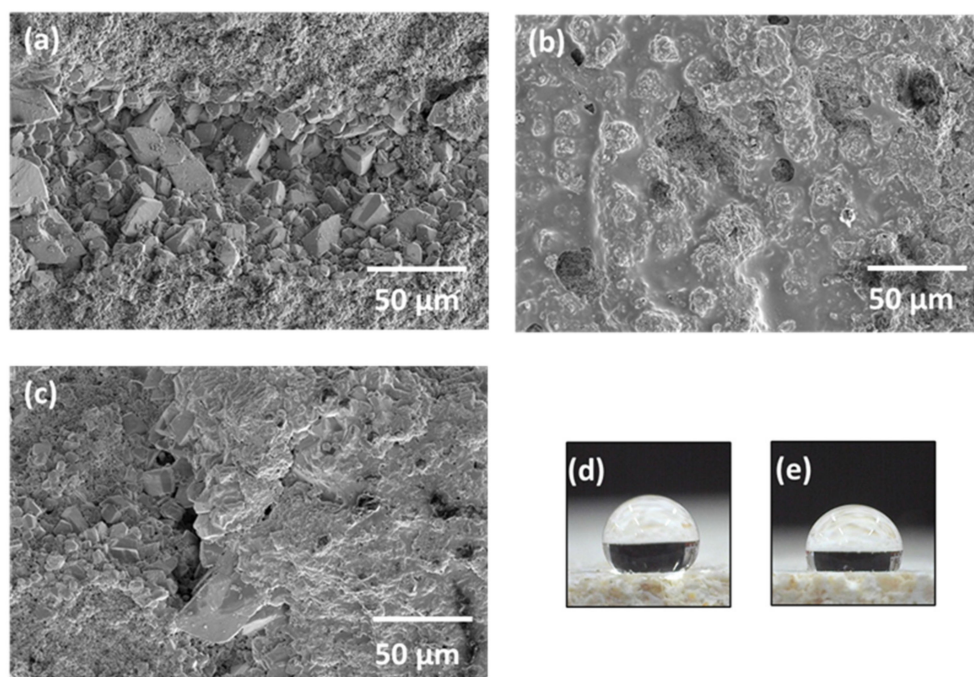


Figure 4. SEM Micrographs of untreated VS (a) compared with coatings with E (b) and NR (c) products. In addition, (d,e) report micro-photos captured for contact angle measurements for samples coated with E and NR, respectively.

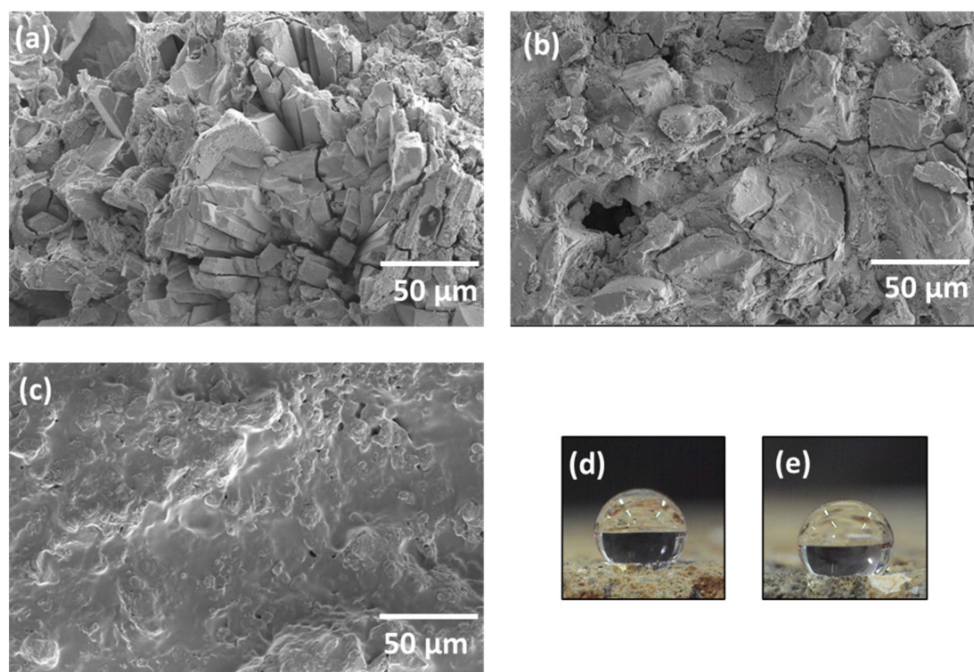


Figure 5. SEM images for (a) pristine T, coated samples with E (b) and NR (c) products. In addition, (d,e) report micro-photos captured during contact angle measurements for samples coated with E and NR, respectively.

When this stone is treated with E (Figure 4b), the morphology shows only on a part of the surface the presence of a veil, uneven, with pores in evidence, created by the coating itself. Observing the treatment with NR (Figure 4c), the material seems to maintain almost unchanged morphology, as the calcite crystals are visible on the surface. The morphology of T (Figure 5) shows irregular crystals well evident (Figure 5a), with anti-graffiti E becoming completely submerged by a crust coating (Figure 5b) that forms pores, not deriving from the underlying substrate. Finally, with NR (Figure 5c) the surface appears quite smooth, even more modified.

The results obtained from microscopic observation are in line with the measurement of the contact angle (θ), i.e., the angle between the surface of the liquid and the outline of the contact surface [28], useful to measure the wettability of T and VS samples coated with E and NR. In the case of water, a surface can be classified as super hydrophilic ($\theta \approx 0^\circ$), hydrophilic ($\theta < 90^\circ$) and hydrophobic ($\theta > 90^\circ$) [37]. Using distilled water, a contact angle of $140.8^\circ \pm 0.5^\circ$ was evaluated for the VS support coated with E product (Figure 4), indicating the super-hydrophobic nature of this surface, since the contact angle is very close to 150° . This result is due to the hierarchical surface texture and roughness of VS surface, which is still preserved after the treatment with E (see Figure 4c,e). In agreement with the Cassie–Baxter model, the maximum contact angle of a water droplet on a non-textured surface is about 130° , while higher contact angles can be achieved only if the surface is rough [37–40]. A contact angle of $121.3^\circ \pm 0.7^\circ$ was evaluated for the deposition of NR on VS, indicating a highly hydrophobic surface. In fact, this surface cannot be classified as super-hydrophobic because of the formation of a non-textured surface, showing a low degree of roughness (Figure 4). In contrast with E, the epoxy resin present in NR seems to modify the morphology of the VS surface, and it caused it to lose its hierarchical structure. The good performances of E may be also due to the contribution of halogen-containing silane agents, which strongly promote the increase of contact angle, especially in the presence of a rough surface (see Section 3.1). Silane agents are in both anti-graffiti products, though a proper surface morphology is essential to obtain high θ values. The surface of the T sample shows smooth pillars responsible for a hierarchical texture and high roughness (Figure 5) [15,41,42]. The high pillar density of this surface allows it to achieve contact

angles near the super-hydrophobic threshold value for samples coated with E and NR, i.e., $140.7^\circ \pm 0.4^\circ$ and $137.9^\circ \pm 0.8^\circ$ respectively (Figure 5b,d). We hypothesize that in the case of the VS the lower contact angle observed for NR indicates that the resin fills the pores of the surface more efficiently, making it smoother compared to the E product (Figure 4b,d). The pillar morphology of T allows it to trap air in the microgrooves of the rough surface so that water droplets lay on a composite surface formed by air and the tops of micro-protrusions, leading to a morphology more suitable to ensure very low area fractions of the solid-liquid interface than that observed for VS [37–39]. In summary, both NR and E formulations, containing silica nanoparticles bounded to the epoxy matrices, allow the suitable nanometric roughness that combined with the VS and T morphologies lead to hierarchical surface textures [43]. In our study, E shows better performance than NR product for both investigated stone materials, conferring higher surface hydrophobicity.

3.4. Water Absorption by Pipe Method

Low-pressure water absorption tests on T and VS materials before and after the treatment with the anti-graffiti were performed (Figure 6).

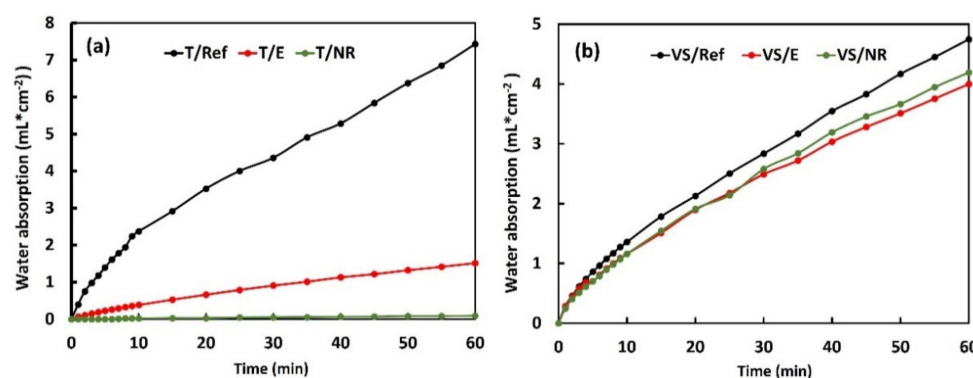


Figure 6. Water absorption by pipe method of T (a) and VS (b): reference sample (black line), after coating with E (red line) and NR (dark green line).

As shown in Figure 6, the T without treatments have an increasing trend of water absorption with a value of 7.4 mL/cm^2 after 60 min. When it is coated with E anti-graffiti, the surface becomes quite waterproof, as the absorption value decreases to 1.5 mL/cm^2 and even more after NR treatment (0.09 mL/cm^2). VS has a porosity less than T and absorbs even less water. In this case, the water absorption value is 4.7 mL/cm^2 after 60 min. Here the anti-graffiti product seems less efficient: in fact, with E and NR the water absorption values are respectively 4.0 and 4.2 mL/cm^2 (NR is slightly higher than E). These results are fully in line with the SEM results and the measured static contact angles: the T treated with the same anti-graffiti of VS becomes more waterproof to water and perhaps even more oleophobic, because its irregular and wrinkly morphology becomes more uniform with the anti-scratch E and even smoother with NR, allowing it to obtain contact angles close to the threshold of super-hydrophobicity higher than VS. As emerged by SEM analysis of VS, E forms a film (Figure 4b) that appears not uniform but porous, allowing penetration of water (but also sprays and markers) into the accessible pores. NR when applied onto VS (Figure 4c) leaves the material morphology almost unaltered. This explains the similar trends observed in the water absorption graphs for E and NR. From the above findings, it is reasonable to expect a higher cleaning efficacy for the T surface when compared to VS. In addition, the treatment with E seems to operate more effectively than NR. All the above hypotheses were confirmed in the cleaning tests as explained below.

3.5. Cleaning Test

An accurate microphotographic report has been performed that showed the effectiveness of protection of E and NR and the removal efficiency of graffiti paints on T (Figure 7)

and VS (Figure 8). In summary, the sprays Motip Dupli black and blue are indicated with the initials S1 and S2, the bitumen spray Montana Cans with S3 and the bitumen marker Molotow with M. We observed, in order, a first group of pictures representing the untreated T, followed by a second group with this material treated with E (indicated with ES1, ES2, ES3 and EM) and finally a third group corresponding to the coating with NR (NRS1, NRS2, NRS3 and NRM). The initials T0, T1 and T2 indicate the number of cleaning cycles. These acronyms have been adopted both for T and for VS. In the case of T, as shown in Figure 7, we observed a gradual spray fading on the untreated T, passing from T0 to T2, with this effect being more evident in the case of anti-graffiti coating. As it can be observed in the same figure, E coating furnishes the best results. In fact, in this case the sprays were almost fully removed, even if the marker cleaning was only partially wiped. On the other hand, with NR coating we observed only a discoloration of both sprays and markers, but no complete or partial removal was achieved.

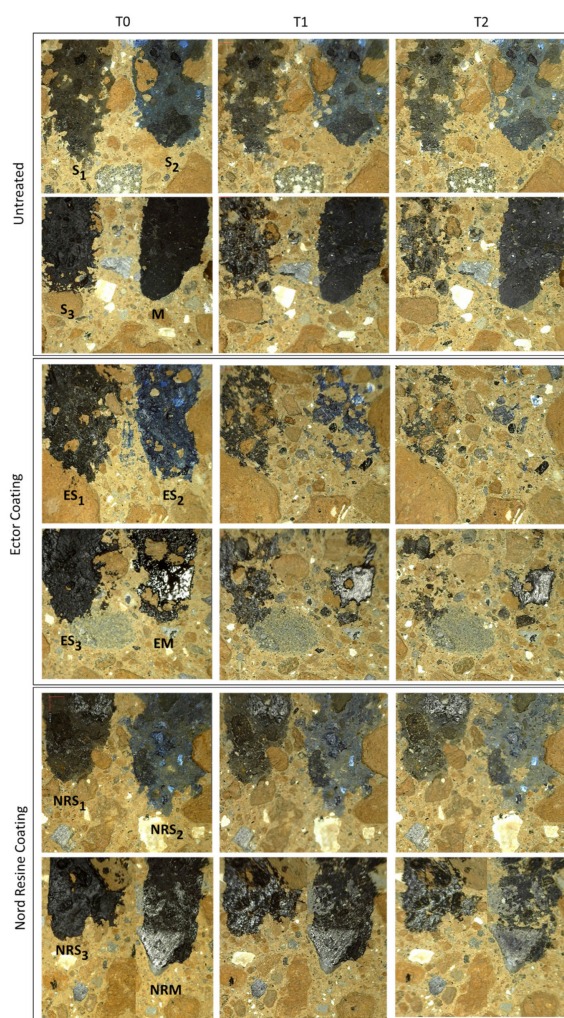


Figure 7. Digital pictures of the cleaning tests performed on T according to the technical sheets: samples not cleaned (T0), and after one (T1) and two (T2) cleaning treatments. Graffiti paints are indicated with the initials S1, S2, S3 and M; ES1, ES2, ES3, and EM indicate the material treated with E. NRS1, NRS2, NRS3 and NRM are the NR treatments.

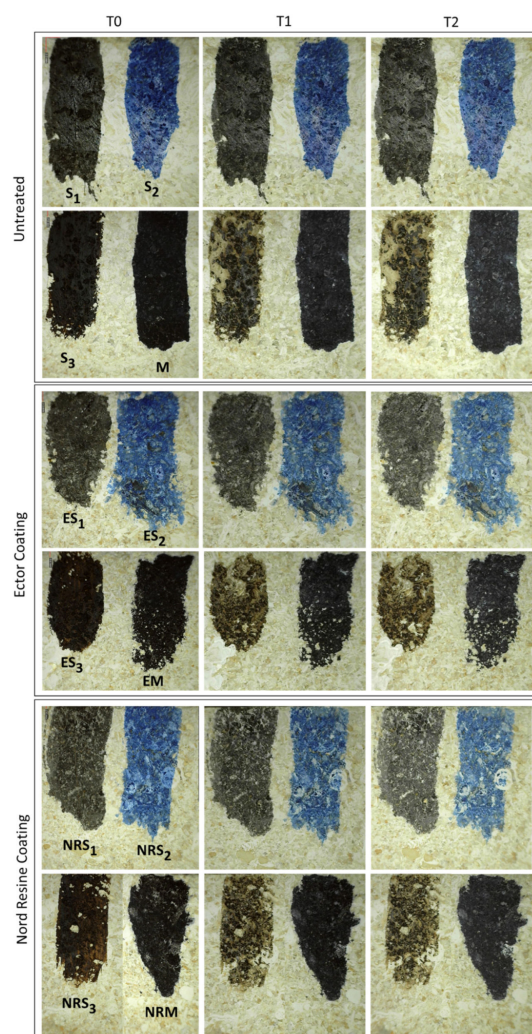


Figure 8. Digital pictures of the cleaning tests performed on VS according to the technical sheets: samples not cleaned (T0), and after one (T1) and two (T2) cleaning treatments. Graffiti paints indicated with the initials S1, S2, S3 and M; ES1, ES2, ES3, and EM indicate the material treated with E. NRS1, NRS2, NRS3, and NRM are the NR treatments.

This behavior is consistent with previous results and suggests a likely more noticeable oleophobicity in E coating than NR. In addition, the test carried out with E treatment demonstrates that even the use of only hot water can be an effective and sustainable method of removal of spray paints and bituminous markers, already at the second cycle of cleaning. Moreover, the use of an ecological product such as E, shows the feasibility of tackling the problem of vandal graffiti with an environmentally friendly product, not harmful to human health. Only a gradual and slight fading, no removal, occurs in the case of VS (Figure 8) and it is more evident only for the S3 bituminous spray that begins to be removed already on the untreated material and gradually fades on the stone with E and NR treatment. All sprays and markers were found to be more dispersed and displayed irregular borders on treated VS when compared to the untreated material, suggesting that the coating was present, but its applied quantity was not enough to ensure the desired results. The scarce efficacy of these commercial products on VS emerged also from the water absorption tests conducted at low pressure (Figure 6) as well from SEM analysis (Figure 4), as discussed previously. This could depend on the scarce absorption of E and NR by VS or on the inadequacy of the cleaning methods. To better understand this phenomenon the materials were weighed before and after treatment with anti-graffiti products, and the percentage of product absorbed was determined. The T treated with E absorbed 0.13%,

while with NR it absorbed almost the double, 0.24%. The VS, even less porous, absorbed only 0.05% when treated with E, while still the double quantity with NR (0.10%). Although the stone materials have different characteristics, the quantity of product NR absorbed was always double compared to E, because it has been applied first diluted 1:1 and then concentrated (as described in Section 2.2). However, in both cases the coatings were very thin, but in the case of T, they guaranteed an effective cleaning (with E) compared to the VS, on which probably a treatment either with several brush hands or with roller or spray could have had a different effect. There are, however, doubts about the effectiveness of the cleaning method on VS: given the delicacy of the stone it was not possible to use harder bristle brushes or more aggressive methods that could damage it.

4. Conclusions

In this study we analyzed the protective effects of two commercial anti-graffiti products, E and NR, on the surface of porous natural stone materials and their morphological characteristics. The anti-graffiti product E, a nanotechnological and environmentally sustainable product, has remarkable effects on the morphology of the treated stone materials, making them repellent to graffiti paints due to its high hydrophobicity. The beneficial action of E allows the easy cleaning of very porous building materials, such as tuff, damaged by vandal graffiti by the warm water method. However, the permanent character of this product hinders its application to the cultural heritage protection. The anti-graffiti NR provides a lower protection than E on both natural porous materials investigated (tuff and Vicenza Stone), even though its semi-sacrificial character makes it suitable for cultural heritage applications, according to the requirements of Italian Ministry for Cultural Heritage and Activities and for Tourism. Overall, the results of this study highlight the importance of developing new anti-graffiti formulations endowed with both the hydrophobicity and the environmental sustainability of E and the sacrificial properties of NR, always keeping great attention on ecologic aspects of the products and their safety toward human health. Finally, new experiments as well the design of innovative and safe cleaning methodologies are planned by us on other porous materials of interest for cultural heritage.

Supplementary Materials: The following supporting information can be downloaded at: <https://www.mdpi.com/article/10.3390/su14010575/s1>, Figure S1: High-magnification SEM micrographs (10 μ m) of untreated VS (a) compared with coatings with E (b) and NR (c) products; Figure S2: High-magnification SEM micrographs (10 μ m) of untreated T (a) compared with coatings with E (b) and NR (c) products.

Author Contributions: V.R., B.L., A.C.: conceptualization, literature collection, samples analysis, writing; V.R., A.B., B.L., F.I., A.C.: data analysis and editing; D.C., A.A.: reviewing of the article. All authors have read and agreed to the published version of the manuscript.

Funding: This research received no external funding.

Institutional Review Board Statement: Not applicable.

Informed Consent Statement: Not applicable.

Acknowledgments: We are grateful to the Department of Chemical Science of Naples for the use of the Scanning Electron Microscopy (SEM).

Conflicts of Interest: The authors declare no conflict of interest.

References

1. Minoletti, F. Profiling, I Profili Dell'Abuso, Il Graffitiismo Vandalico. In *Crimine & Società*, 3rd ed.; Giornale Scientifico a Cura dell'Osservatorio Nazionale Abusi Psicologici: Florence, Italy, 2017.
2. Sanmartín, P.; Cappitelli, F.; Mitchell, R. Current methods of graffiti removal: A review. *Constr. Build. Mater.* **2014**, *71*, 363–374. [[CrossRef](#)]
3. Giorgi, R.; Baglioni, M.; Baglioni, P. Nanofluids and chemical highly retentive hydrogels for controlled and selective removal of overpaintings and undesired graffiti from street art. *Anal. Bioanal. Chem.* **2017**, *409*, 3707–3712. [[CrossRef](#)]

4. Baglioni, M.; Poggi, G.; Benavides, Y.J.; Camacho, F.M.; Giorgi, R.; Baglioni, P. Nanostructured fluids for the removal of graffiti—A survey on 17 commercial spray-can paints. *J. Cult. Herit.* **2018**, *34*, 218–226. [\[CrossRef\]](#)
5. Circular, No. 92 of the Ministry of Cultural Heritage and Activities, Actions to Prevent Damage to Architectural Surfaces by Graphic Vandalism. 2003. Available online: http://win.unsabeniculturali.it/pdf/2003/092_2003.pdf (accessed on 29 November 2021).
6. Samolik, S.; Walczak, M.; Plotek, M.; Sarzynski, A.; Pluska, I.; Marczak, J. Investigation into the removal of graffiti on mineral supports: Comparison of nano-second Nd:YAG laser cleaning with traditional mechanical and chemical methods. *Stud. Conserv.* **2015**, *60*, S58–S64. [\[CrossRef\]](#)
7. Carvalh o, M.; Dion sio, A. Evaluation of mechanical soft-abrasive blasting and chemical cleaning methods on alkyd-paint graffiti made on calcareous stones. *J. Cult. Herit.* **2015**, *16*, 579–590. [\[CrossRef\]](#)
8. Pozo-Antonio, J.S.; L pez, L.; Dion sio, A.; Rivas, T. A Study on the Suitability of Mechanical Soft-Abrasive Blasting Methods to Extract Graffiti Paints on Ornamental Stones. *Coatings* **2018**, *8*, 335. [\[CrossRef\]](#)
9. Ranalli, G.; Belli, C.; Alfano, G.; Lustrato, G.; Zanardini, E.; Cappitelli, F.; Sorlini, C. Bio-cleaning of cultural heritage surfaces: Biotechnological contributions, Bioremediation of works of art. *Househ Pers Care Today* **2009**, *3*, 36–39.
10. Ranalli, G.; Zanardini, E. Biocleaning on Cultural Heritage: New frontiers of microbial biotechnologies. *J. Appl. Microbiol.* **2021**, *131*, 583–603. [\[CrossRef\]](#)
11. Troiano, F.; Vicini, S.; Giovent , E.; Lorenzi, P.F.; Improta, C.M.; Cappitelli, F. A methodology to select bacteria able to remove synthetic polymers. *Polym. Degrad. Stab.* **2014**, *107*, 321–327. [\[CrossRef\]](#)
12. Prati, S.; Volpi, F.; Fontana, R.; Galletti, P.; Giorgini, L.; Mazzeo, R.; Mazzocchetti, L.; Samor , C.; Sciutto, G.; Tagliavini, E. Sustainability in art conservation: A novel bio-based organogel for the cleaning of water sensitive works of art. *Pure Appl. Chem.* **2018**, *2*, 239–251. [\[CrossRef\]](#)
13. Zhong, X.; Hu, H.; Yang, L.; Sheng, J.; Fu, H. Robust Hyperbranched Polyester-Based Anti-Smudge Coatings for Self-Cleaning, Anti-graffiti, and Chemical Shielding. *Appl. Mat. Interfaces* **2019**, *11*, 14305–14312. [\[CrossRef\]](#)
14. Lettieri, M.; Masieri, M.; Pipoli, M.; Morelli, A.; Frigione, M. Anti-graffiti Behavior of Oleo/Hydrophobic Nano-Filled Coatings Applied on Natural Stone Materials. *Coatings* **2019**, *9*, 740. [\[CrossRef\]](#)
15. D’Arienzo, L.; Scarfato, P.; Incarnato, L. New polymeric nanocomposites for improving the protective and consolidating efficiency of tuff stone. *J. Cult. Herit.* **2008**, *9*, 253–260. [\[CrossRef\]](#)
16. Iucolano, F.; Colella, A.; Liguori, B.; Calcaterra, D. Suitability of silica nanoparticles for tuff consolidation. *Constr. Build. Mater.* **2019**, *202*, 73–81. [\[CrossRef\]](#)
17. Pargoletti, E.; Comite, V.; Fermo, P.; Sabatini, V.; Cappelletti, G. Enhanced Historical Limestone Protection by New Organic/Inorganic Additive-Modified Resins. *Coatings* **2021**, *11*, 73. [\[CrossRef\]](#)
18. Moura, A.; Flores-Colen, I.; de Brito, J.; Dion sio, A. Study of the cleaning effectiveness of limestone and lime-based mortar substrates protected with anti-graffiti products. *J. Cult. Herit.* **2017**, *24*, 31–44. [\[CrossRef\]](#)
19. Novembre, D.; Gimeno, D.; Cappelletti, P.; Graziano, S.F. A case study of zeolitization process: “Tufo Rosso a Scorie Nere” (Vico volcano, Italy): Inferences for a general model. *Eur. J. Mineral.* **2021**, *33*, 315–328. [\[CrossRef\]](#)
20. Di Benedetto, C.; Cappelletti, P.; Favaro, M.; Graziano, S.F.; Langella, A.; Calcaterra, D.; Colella, A. Porosity as key factor in the durability of two historical building stones: Neapolitan Yellow Tuff and Vicenza Stone. *Eng. Geol.* **2015**, *193*, 310–319. [\[CrossRef\]](#)
21. Scrivano, S.; Gaggero, L.; Gisbert Aguilar, J. Micro-porosity and mineral-petrographic features influences on decay: Experimental data from four-dimension stones. *Constr. Build. Mater.* **2018**, *173*, 342–349. [\[CrossRef\]](#)
22. Scrivano, S.; Gaggero, L.; Gisbert Aguilar, J. An Experimental Investigation of the Effects of Grain Size and Pore Network on the Durability of Vicenza Stone. *Rock Mech. Rock Eng.* **2019**, *52*, 2935–2948. [\[CrossRef\]](#)
23. Regulation (EC), No. 1272/2008 of the European Parliament and of the Council of 16 December 2008 on the Classification, Labelling and Packaging of Substances and Mixtures, Amending and Repealing Directives 67/548/EEC and 1999/45/EC and Amending Regulation (EC) No. 1907/2006 (Text with EEA Relevance). Available online: <https://eur-lex.europa.eu/eli/reg/2008/1272/oj> (accessed on 29 November 2021).
24. UNI EN 16302, Conservation of Cultural Heritage—Test Methods—Measurement of Water Absorption by Pipe Method. 2013. Available online: <https://standards.iteh.ai/catalog/standards/cen/530acec8-63ad-48c3-87a9-ab63853b9d2b/en-16302-2013> (accessed on 29 November 2021).
25. Colella, A.; Capasso, I.; Iucolano, F. Comparison of Latest and Innovative Silica-Based Consolidants for Volcanic Stones. *Materials* **2021**, *14*, 2513. [\[CrossRef\]](#) [\[PubMed\]](#)
26. UNI EN 15886, Conservation of Cultural Property—Test Methods—Color Measurement of Surfaces. 2010. Available online: <https://standards.iteh.ai/catalog/standards/cen/048ec4b9-497e-42d0-b653-a5a8d075815e/en-15886-2010> (accessed on 29 November 2021).
27. Rodrigues, J.D.; Grossi, A. Indicators and ratings for the compatibility assessment of conservation actions. *J. Cult. Herit.* **2007**, *8*, 32–43. [\[CrossRef\]](#)
28. UNI EN 15802, Conservation of Cultural Property—Test Methods—Static Contact Angle Determinations. 2010. Available online: <https://standards.iteh.ai/catalog/standards/cen/a93aafde-6380-4bc5-9d9b-d3b535dee619/en-15802-2009> (accessed on 29 November 2021).
29. Randle, R.R.; Whiffen, D.H. The infra-red intensities of a band near 1020 cm^{−1} in mono- and para-substituted benzene derivatives. *Trans. Faraday Soc.* **1956**, *52*, 9–13. [\[CrossRef\]](#)

30. Braatz, D.A.; Antonio, M.R.; Nilsson, M. Structural study of complexes formed by acidic and neutral organophosphorus reagents. *Dalton. Trans.* **2017**, *46*, 1194–1206. [[CrossRef](#)] [[PubMed](#)]
31. Bifulco, A.; Parida, D.; Khalifah, A.S.; Nazir, R.; Lehner, S.; Stämpfli, R.; Markus, H.; Malucelli, G.; Branda, F.; Gaan, S. Fire and mechanical properties of DGEBA-based epoxy resin cured with a cycloaliphatic hardener: Combined action of silica, melamine and DOPO-derivative. *Mater. Des.* **2020**, *193*, 108862. [[CrossRef](#)]
32. Bukalo, N.N.; Ekosse, G.E.; Odiyo, J.O.; Ogola, J.S. Fourier Transform Infrared Spectroscopy of Clay Size Fraction of Cretaceous-Tertiary Kaolins in the Douala Sub-Basin, Cameroon. *Open Geosci.* **2017**, *9*, 407–418. [[CrossRef](#)]
33. Bifulco, A.; Marotta, A.; Passaro, J.; Costantini, A.; Cerruti, P.; Gentile, G.; Ambrogio, V.; Malucelli, G.; Branda, F. Thermal and Fire Behavior of a Bio-Based Epoxy/Silica Hybrid Cured with Methyl Nadic Anhydride. *Polymers* **2020**, *12*, 1661. [[CrossRef](#)]
34. Joseph, T.; Varghese, H.T.; Panicker, C.Y.; Viswanathan, K.; Dolezal, M.; Van Alsenoy, C. Spectroscopic (FT-IR, FT-Raman), first order hyperpolarizability, NBO analysis, HOMO and LUMO analysis of N-[(4-(trifluoromethyl) phenyl] pyrazine-2-carboxamide by density functional methods. *Arab. J. Chem.* **2017**, *10*, S2281–S2294. [[CrossRef](#)]
35. Sainan, X.; Junyan, Y.; Han, Z.; Decheng, F.; Zhaoyuan, S. Micromorphology and Micromechanical Properties Evolution of Bitumen and Bitumen Fractions Using Atomic Force Microscopy Considering Temperature Effect. *Energy Fuels* **2021**, *35*, 17434–17445. [[CrossRef](#)]
36. Zendri, E.; Biscontin, G.; Kosmidis, P. Effects of condensed water on limestone surfaces in a marine environment. *J. Cult. Herit.* **2001**, *2*, 283–289. [[CrossRef](#)]
37. Kota, A.; Kwon, G.; Tuteja, A. The design and applications of superomniphobic surfaces. *NPG Asia Mater.* **2014**, *6*, e109. [[CrossRef](#)]
38. Koch, K.; Bhushan, B.; Jung, Y.C.; Barthlot, W. Fabrication of artificial Lotus leaves and significance of hierarchical structure for superhydrophobicity and low adhesion. *Soft Matter* **2009**, *5*, 1386–1393. [[CrossRef](#)]
39. Xue, C.H.; Jia, S.T.; Zhang, J.; Ma, J.Z. Large-area fabrication of superhydrophobic surfaces for practical applications: An overview. *Sci. Technol. Adv. Mater.* **2010**, *11*, 3. [[CrossRef](#)]
40. Pota, G.; Bifulco, G.; Parida, D.; Zhao, S.; Rentsch, D.; Amendola, E.; Califano, V.; Costantini, A. Tailoring the hydrophobicity of wrinkled silica nanoparticles and of the adsorption medium as a strategy for immobilizing lipase: An efficient catalyst for biofuel production. *Microporous Mesoporous Mater.* **2021**, *328*, 111504. [[CrossRef](#)]
41. Vacchiano, C.; Incarnato, L.; Scarfato, P.; Acierno, D. Conservation of tuff-stone with polymeric resins. *Constr. Build. Mater.* **2008**, *22*, 855–865. [[CrossRef](#)]
42. Tesser, E.; Lazzarini, L.; Bracci, S. Investigation on the chemical structure and ageing transformations of the cycloaliphatic epoxy resin EP2101 used as stone consolidant. *J. Cult. Herit.* **2017**, *31*, 72–82. [[CrossRef](#)]
43. Avossa, J.; Bifulco, A.; Amendola, E.; Gesuele, F.; Oscurato, S.L.; Gizaw, Y.; Mensitieri, G.; Branda, F. Forming nanostructured surfaces through Janus colloidal silica particles with nanowrinkles: A new strategy to superhydrophobicity. *Appl. Surf. Sci.* **2019**, *465*, 73–81. [[CrossRef](#)]